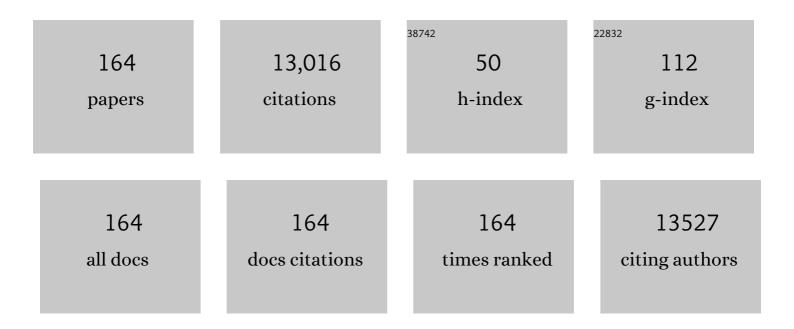
List of Publications by Year in descending order

Source: https://exaly.com/author-pdf/3909695/publications.pdf Version: 2024-02-01



#	Article	IF	CITATIONS
1	Present and Future of Surface-Enhanced Raman Scattering. ACS Nano, 2020, 14, 28-117.	14.6	2,153
2	Plasmonics for future biosensors. Nature Photonics, 2012, 6, 709-713.	31.4	919
3	A review on the fabrication of substrates for surface enhanced Raman spectroscopy and their applications in analytical chemistry. Analytica Chimica Acta, 2011, 693, 7-25.	5.4	905
4	Surface Plasmon Sensor Based on the Enhanced Light Transmission through Arrays of Nanoholes in Gold Films. Langmuir, 2004, 20, 4813-4815.	3.5	715
5	A New Generation of Sensors Based on Extraordinary Optical Transmission. Accounts of Chemical Research, 2008, 41, 1049-1057.	15.6	492
6	Strong Polarization in the Optical Transmission through Elliptical Nanohole Arrays. Physical Review Letters, 2004, 92, 037401.	7.8	439
7	Nanohole-Enhanced Raman Scattering. Nano Letters, 2004, 4, 2015-2018.	9.1	418
8	A review on recent advances in the applications of surface-enhanced Raman scattering in analytical chemistry. Analytica Chimica Acta, 2020, 1097, 1-29.	5.4	339
9	Increased cut-off wavelength for a subwavelength hole in a real metal. Optics Express, 2005, 13, 1933.	3.4	283
10	Nanoholes As Nanochannels: Flow-through Plasmonic Sensing. Analytical Chemistry, 2009, 81, 4308-4311.	6.5	264
11	On-Chip Surface-Based Detection with Nanohole Arrays. Analytical Chemistry, 2007, 79, 4094-4100.	6.5	258
12	Probing Dynamic Generation of Hot-Spots in Self-Assembled Chains of Gold Nanorods by Surface-Enhanced Raman Scattering. Journal of the American Chemical Society, 2011, 133, 7563-7570.	13.7	251
13	Silver nanoparticles self assembly as SERS substrates with near single molecule detection limit. Physical Chemistry Chemical Physics, 2009, 11, 7381.	2.8	224
14	Enhanced Fluorescence from Arrays of Nanoholes in a Gold Film. Journal of the American Chemical Society, 2005, 127, 14936-14941.	13.7	203
15	Structural Investigation of MFe <sub>2</sub> O <sub>4</sub> (M = Fe, Co) Magnetic Fluids. Journal of Physical Chemistry C, 2009, 113, 7684-7691.	3.1	199
16	Periodic Metallic Nanostructures as Plasmonic Chemical Sensors. Langmuir, 2013, 29, 5638-5649.	3.5	189
17	Surface-enhanced Raman scattering (SERS) from Au:Ag bimetallic nanoparticles: the effect of the molecular probe. Chemical Science, 2013, 4, 509-515.	7.4	183
18	Attomolar Protein Detection Using in-Hole Surface Plasmon Resonance. Journal of the American Chemical Society, 2009, 131, 436-437.	13.7	131

#	Article	IF	CITATIONS
19	High-performance microfluidic vanadium redox fuel cell. Electrochimica Acta, 2007, 52, 4942-4946.	5.2	127
20	Largeâ€Area Fabrication of Periodic Arrays of Nanoholes in Metal Films and Their Application in Biosensing and Plasmonicâ€Enhanced Photovoltaics. Advanced Functional Materials, 2010, 20, 3918-3924.	14.9	125
21	Multilayer silver nanoparticles-modified optical fiber tip for high performance SERS remote sensing. Biosensors and Bioelectronics, 2010, 25, 2270-2275.	10.1	123
22	Optofluidic Concentration: Plasmonic Nanostructure as Concentrator and Sensor. Nano Letters, 2012, 12, 1592-1596.	9.1	121
23	Hydrogen Peroxide as an Oxidant for Microfluidic Fuel Cells. Journal of the Electrochemical Society, 2007, 154, B1220.	2.9	115
24	High-speed imaging of surface-enhanced Raman scattering fluctuations from individual nanoparticles. Nature Nanotechnology, 2019, 14, 981-987.	31.5	115
25	Applications of surface enhanced Raman scattering to the study of metal-adsorbate interactions. Journal of Molecular Structure, 1997, 405, 29-44.	3.6	111
26	Silver Nanoparticles on a Plastic Platform for Localized Surface Plasmon Resonance Biosensing. Analytical Chemistry, 2010, 82, 6350-6352.	6.5	107
27	Flow-Through vs Flow-Over: Analysis of Transport and Binding in Nanohole Array Plasmonic Biosensors. Analytical Chemistry, 2010, 82, 10015-10020.	6.5	103
28	Investigation of the Adsorption ofl-Cysteine on a Polycrystalline Silver Electrode by Surface-Enhanced Raman Scattering (SERS) and Surface-Enhanced Second Harmonic Generation (SESHG). Journal of Physical Chemistry B, 2002, 106, 5982-5987.	2.6	102
29	Nanoparticle-Containing Structures as a Substrate for Surface-Enhanced Raman Scattering. Langmuir, 2006, 22, 8696-8702.	3.5	100
30	Variability in Raman Spectra of Single Human Tumor Cells Cultured <i>in vitro</i> : Correlation with Cell Cycle and Culture Confluency. Applied Spectroscopy, 2010, 64, 871-887.	2.2	99
31	Apex-Enhanced Raman Spectroscopy Using Double-Hole Arrays in a Gold Film. Journal of Physical Chemistry C, 2007, 111, 2347-2350.	3.1	96
32	Nanohole arrays in metal films as optofluidic elements: progress and potential. Microfluidics and Nanofluidics, 2008, 4, 107-116.	2.2	79
33	Intensity Fluctuations in Single-Molecule Surface-Enhanced Raman Scattering. Accounts of Chemical Research, 2019, 52, 456-464.	15.6	76
34	Significant Suppression of Spontaneous Emission in SiO2Photonic Crystals Made with Tb3+-Doped LaF3Nanoparticles. Journal of Physical Chemistry C, 2007, 111, 4047-4051.	3.1	73
35	Surfaceâ€enhanced Raman scattering from polystyrene on gold clusters. Journal of Raman Spectroscopy, 2010, 41, 745-751.	2.5	72
36	Adsorption/desorption behaviour of cysteine and cystine in neutral and basic media: electrochemical evidence for differing thiol and disulfide adsorption to a Au(111) single crystal electrode. Journal of Electroanalytical Chemistry, 2003, 550-551, 291-301.	3.8	71

#	Article	IF	CITATIONS
37	The orientation of 2,2′-bipyridine adsorbed at a SERS-active Au(111) electrode surface. Journal of Electroanalytical Chemistry, 2003, 547, 163-172.	3.8	70
38	Determination of aqueous antibiotic solutions using SERS nanogratings. Analytica Chimica Acta, 2017, 982, 148-155.	5.4	70
39	Ratio of the surface-enhanced anti-Stokes scattering to the surface-enhanced Stokes-Raman scattering for molecules adsorbed on a silver electrode. Physical Review B, 2004, 69, .	3.2	69
40	Side-by-Side Assembly of Gold Nanorods Reduces Ensemble-Averaged SERS Intensity. Journal of Physical Chemistry C, 2012, 116, 5538-5545.	3.1	67
41	Basis and Lattice Polarization Mechanisms for Light Transmission through Nanohole Arrays in a Metal Film. Nano Letters, 2005, 5, 1243-1246.	9.1	66
42	Improved Synthesis of Gold and Silver Nanoshells. Langmuir, 2013, 29, 4366-4372.	3.5	66
43	Surface Plasmonâ^'Quantum Dot Coupling from Arrays of Nanoholes. Journal of Physical Chemistry B, 2006, 110, 8307-8313.	2.6	64
44	Digital Protocol for Chemical Analysis at Ultralow Concentrations by Surface-Enhanced Raman Scattering. Analytical Chemistry, 2018, 90, 1248-1254.	6.5	63
45	Localized Raman Enhancement from a Double-Hole Nanostructure in a Metal Film. Journal of Physical Chemistry C, 2008, 112, 15098-15101.	3.1	62
46	Electrochemical Control of the Time-Dependent Intensity Fluctuations in Surface-Enhanced Raman Scattering (SERS). Journal of Physical Chemistry C, 2009, 113, 17737-17744.	3.1	62
47	Biochemical signatures of <i>in vitro</i> radiation response in human lung, breast and prostate tumour cells observed with Raman spectroscopy. Physics in Medicine and Biology, 2011, 56, 6839-6855.	3.0	58
48	Quantification of ovarian cancer markers with integrated microfluidic concentration gradient and imaging nanohole surface plasmon resonance. Analyst, The, 2013, 138, 1450.	3.5	58
49	Raman spectroscopy identifies radiation response in human non-small cell lung cancer xenografts. Scientific Reports, 2016, 6, 21006.	3.3	57
50	Zika Immunoassay Based on Surface-Enhanced Raman Scattering Nanoprobes. ACS Sensors, 2018, 3, 587-594.	7.8	57
51	Surface-enhanced Raman scattering (SERS) optrodes for multiplexed on-chip sensing of nile blue A and oxazine 720. Lab on A Chip, 2012, 12, 1554.	6.0	49
52	Enhanced Raman Scattering from Nanoholes in a Copper Film. Journal of Physical Chemistry C, 2008, 112, 17051-17055.	3.1	48
53	Ag decorated sandpaper as flexible SERS substrate for direct swabbing sampling. Materials Letters, 2014, 133, 57-59.	2.6	48
54	Tuning Gold Nanoparticle Self-Assembly for Optimum Coherent Anti-Stokes Raman Scattering and Second Harmonic Generation Response. Journal of Physical Chemistry C, 2009, 113, 3586-3592.	3.1	44

#	Article	IF	CITATIONS
55	Microfluidic Plasmonic Biosensor for Breast Cancer Antigen Detection. Plasmonics, 2016, 11, 45-51.	3.4	44
56	Selfâ€Assembled Au Nanoparticles as Substrates for Surfaceâ€Enhanced Vibrational Spectroscopy: Optimization and Electrochemical Stability. ChemPhysChem, 2008, 9, 1899-1907.	2.1	43
57	Effect of periodicity on the performance of surface plasmon resonance sensors based on subwavelength nanohole arrays. Sensors and Actuators B: Chemical, 2013, 178, 366-370.	7.8	43
58	Integrated nanohole array surface plasmon resonance sensing device using a dual-wavelength source. Journal of Micromechanics and Microengineering, 2011, 21, 115001.	2.6	41
59	Statistical Correlation Between SERS Intensity and Nanoparticle Cluster Size. Journal of Physical Chemistry C, 2013, 117, 16596-16605.	3.1	41
60	A silver nanoparticle embedded hydrogel as a substrate for surface contamination analysis by surface-enhanced Raman scattering. Analyst, The, 2014, 139, 5283-5289.	3.5	38
61	Polarization-dependent sensing of a self-assembled monolayer using biaxial nanohole arrays. Applied Physics Letters, 2008, 92, .	3.3	37
62	FTâ€ <b>i</b> R, FTâ€Raman and SERS spectra of anilinium sulfate. Journal of Raman Spectroscopy, 2009, 40, 1810-1815.	2.5	36
63	Mapping the Energy Distribution of SERRS Hot Spots from Anti-Stokes to Stokes Intensity Ratios. Journal of the American Chemical Society, 2012, 134, 13492-13500.	13.7	36
64	Surface-Enhanced Resonance Raman Scattering (SERRS) Using Au Nanohole Arrays on Optical Fiber Tips. Plasmonics, 2013, 8, 1113-1121.	3.4	36
65	Detection of Buried Explosives Using a Surface-Enhanced Raman Scattering (SERS) Substrate Tailored for Miniaturized Spectrometers. ACS Sensors, 2020, 5, 2933-2939.	7.8	36
66	Optimizing Plasmonic Silicon Photovoltaics with Ag and Au Nanoparticle Mixtures. Journal of Physical Chemistry C, 2014, 118, 5889-5895.	3.1	34
67	Protonation and deprotonation of cysteine and cystine monolayers probed by impedance spectroscopy. Journal of Electroanalytical Chemistry, 2009, 625, 109-116.	3.8	31
68	Enhanced performance of dye-sensitized solar cells using gold nanoparticles modified fluorine tin oxide electrodes. Journal Physics D: Applied Physics, 2013, 46, 024005.	2.8	31
69	SERS optrode as a "fishing rod―to direct pre-concentrate analytes from superhydrophobic surfaces. Chemical Communications, 2015, 51, 1965-1968.	4.1	31
70	The electrochemical reduction of CO <sub>2</sub> on a copper electrode in 1- <i>n</i> -butyl-3-methyl imidazolium tetrafluoroborate (BMI.BF <sub>4</sub> ) monitored by surface-enhanced Raman scattering (SERS). Journal of Raman Spectroscopy, 2016, 47, 674-680.	2.5	31
71	A Hierarchical Self-Assembly Route to Three-Dimensional Polymerâ^'Quantum Dot Photonic Arrays. Langmuir, 2007, 23, 5251-5254.	3.5	30
72	<i>Ex Vivo</i> Detection of Circulating Tumor Cells from Whole Blood by Direct Nanoparticle Visualization. ACS Nano, 2018, 12, 1902-1909.	14.6	30

#	Article	IF	CITATIONS
73	Strong Polarized Enhanced Raman Scattering via Optical Tunneling through Random Parallel Nanostructures in Au Thin Films. Journal of Physical Chemistry B, 2005, 109, 401-405.	2.6	28
74	Radiation-Induced Glycogen Accumulation Detected by Single Cell Raman Spectroscopy Is Associated with Radioresistance that Can Be Reversed by Metformin. PLoS ONE, 2015, 10, e0135356.	2.5	28
75	Surface-enhanced Raman scattering (SERS) from a silver electrode modified with oxazine 720. Canadian Journal of Chemistry, 2004, 82, 1474-1480.	1.1	27
76	Plasmonic labeling of subcellular compartments in cancer cells: multiplexing with fine-tuned gold and silver nanoshells. Chemical Science, 2017, 8, 3038-3046.	7.4	27
77	Surface-enhanced Raman scattering from oxazine 720 adsorbed on scratched gold films. Journal of Raman Spectroscopy, 2005, 36, 629-634.	2.5	26
78	Improved Performance of Nanohole Surface Plasmon Resonance Sensors by the Integrated Response Method. IEEE Photonics Journal, 2011, 3, 441-449.	2.0	25
79	Single-Molecule Surface-Enhanced (Resonance) Raman Scattering (SE(R)RS) as a Probe for Metal Colloid Aggregation State. Journal of Physical Chemistry C, 2016, 120, 20877-20885.	3.1	25
80	lmmunoassay quantification using surface-enhanced fluorescence (SEF) tags. Analyst, The, 2017, 142, 2717-2724.	3.5	25
81	Dynamic Imaging of Multiple SERS Hotspots on Single Nanoparticles. ACS Photonics, 2020, 7, 434-443.	6.6	24
82	Using Polycarbonate Membranes as Templates for the Preparation of Au Nanostructures for Surface-Enhanced Raman Scattering. Journal of Nanoscience and Nanotechnology, 2009, 9, 3233-3238.	0.9	21
83	Improving the performance of gold nanohole array biosensors by controlling the optical collimation conditions. Applied Optics, 2015, 54, 6502.	2.1	21
84	Exploring Diffusion and Cellular Uptake: Charged Gold Nanoparticles in an in Vitro Breast Cancer Model. ACS Applied Bio Materials, 2020, 3, 6992-7002.	4.6	21
85	Surface-Enhanced Resonance Raman Scattering on Gold Concentric Rings: Polarization Dependence and Intensity Fluctuations. Journal of Physical Chemistry C, 2012, 116, 2672-2676.	3.1	19
86	Leukemic marker detection using a spectro-polarimetric surface plasmon resonance platform. Biosensors and Bioelectronics, 2015, 63, 80-85.	10.1	19
87	Detection of hydrogen peroxide using an optical fiber-based sensing probe. Sensors and Actuators B: Chemical, 2013, 185, 166-173.	7.8	18
88	Breast cancer subtype specific biochemical responses to radiation. Analyst, The, 2018, 143, 3850-3858.	3.5	18
89	Collagen Type l–Gelatin Methacryloyl Composites: Mimicking the Tumor Microenvironment. ACS Biomaterials Science and Engineering, 2019, 5, 2887-2898.	5.2	18
90	Digital plasmonic holography. Light: Science and Applications, 2018, 7, 52.	16.6	17

#	Article	IF	CITATIONS
91	Fluctuations of the Stokes and anti-Stokes surface-enhanced resonance Raman scattering intensities in an electrochemical environment. Chemical Communications, 2011, 47, 7158.	4.1	16
92	Low-Cost Leukemic Serum Marker Screening Using Large Area Nanohole Arrays on Plastic Substrates. ACS Sensors, 2016, 1, 1103-1109.	7.8	16
93	Raman spectroscopy and group and basis-restricted non negative matrix factorisation identifies radiation induced metabolic changes in human cancer cells. Scientific Reports, 2021, 11, 3853.	3.3	16
94	Comparison of Ag and SiO <sub>2</sub> Nanoparticles for Light Trapping Applications in Silicon Thin Film Solar Cells. Journal of Physical Chemistry Letters, 2014, 5, 3302-3306.	4.6	15
95	Surface plasmon enhanced up-conversion from NaYF <sub>4</sub> :Yb/Er/Gd nano-rods. Physical Chemistry Chemical Physics, 2015, 17, 16170-16177.	2.8	15
96	Use of polarization-dependent SERS from scratched gold films to monitor the electrochemically-driven desorption and readsorption of cysteine. Journal of Electroanalytical Chemistry, 2010, 649, 159-163.	3.8	14
97	Cost-effective nanostructured thin-film solar cell with enhanced absorption. Applied Physics Letters, 2014, 105, .	3.3	14
98	Electrochemical Control of Light Transmission through Nanohole Electrode Arrays. ACS Photonics, 2016, 3, 2375-2382.	6.6	14
99	Light trapping in a-Si:H thin film solar cells using silver nanostructures. AIP Advances, 2017, 7, .	1.3	14
100	Surface-enhanced Raman scattering from bowtie nanoaperture arrays. Surface Science, 2018, 676, 39-45.	1.9	14
101	Monitor Ionizing Radiation-Induced Cellular Responses with Raman Spectroscopy, Non-Negative Matrix Factorization, and Non-Negative Least Squares. Applied Spectroscopy, 2020, 74, 701-711.	2.2	14
102	The Use of Polarization-dependent SERS from Scratched Gold Films to Selectively Eliminate Solution-phase Interference. Plasmonics, 2007, 2, 157-162.	3.4	13
103	Spectroscopic investigations and computational study of sulfur trioxide–pyridine complex. Journal of Raman Spectroscopy, 2011, 42, 1812-1819.	2.5	13
104	Cu nanoparticles enable plasmonic-improved silicon photovoltaic devices. Physical Chemistry Chemical Physics, 2012, 14, 15722.	2.8	13
105	Comparing the Electrochemical Response of Nanostructured Electrode Arrays. Analytical Chemistry, 2017, 89, 6129-6135.	6.5	13
106	Statistics on Surface-Enhanced Resonance Raman Scattering from Single Nanoshells. Journal of Physical Chemistry C, 2011, 115, 19104-19109.	3.1	12
107	Haralick texture feature analysis for quantifying radiation response heterogeneity in murine models observed using Raman spectroscopic mapping. PLoS ONE, 2019, 14, e0212225.	2.5	11
108	Ultra-High-Speed Dynamics in Surface-Enhanced Raman Scattering. Journal of Physical Chemistry C, 2021, 125, 7523-7532.	3.1	11

#	Article	IF	CITATIONS
109	Uncovering the Mechanism for the Formation of Copper Thioantimonate (Sb <sup>V</sup> ) Nanoparticles and Its Transition to Thioantimonide (Sb <sup>III</sup> ). Crystal Growth and Design, 2018, 18, 6521-6527.	3.0	10
110	Comparison of SERS Performances of Co and Ni Ultrathin Films over Silver to Electrochemically Activated Co and Ni Electrodes. Journal of Physical Chemistry C, 2008, 112, 15348-15355.	3.1	9
111	Detecting Antibodies Secreted by Trapped Cells Using Extraordinary Optical Transmission. IEEE Sensors Journal, 2011, 11, 2732-2739.	4.7	9
112	Nanoplasmonic Structures in Optical Fibers. , 2012, , 289-315.		9
113	Polarization-dependent surface-enhanced Raman scattering (SERS) from microarrays. Analytica Chimica Acta, 2017, 972, 73-80.	5.4	9
114	Recessed Gold Nanoring–Ring Microarray Electrodes. Analytical Chemistry, 2017, 89, 9870-9876.	6.5	9
115	Proof of concept for a passive sampler for monitoring of gaseous elemental mercury in artisanal gold mining. Scientific Reports, 2017, 7, 16513.	3.3	9
116	Raman spectroscopy detects metabolic signatures of radiation response and hypoxic fluctuations in non-small cell lung cancer. BMC Cancer, 2019, 19, 474.	2.6	9
117	High-Speed Fluctuations in Surface-Enhanced Raman Scattering Intensities from Various Nanostructures. Applied Spectroscopy, 2020, 74, 1398-1406.	2.2	9
118	Group and Basis Restricted Non-Negative Matrix Factorization and Random Forest for Molecular Histotype Classification and Raman Biomarker Monitoring in Breast Cancer. Applied Spectroscopy, 2022, 76, 462-474.	2.2	9
119	Absorption leads to narrower plasmonic resonances. Journal of the Optical Society of America B: Optical Physics, 2019, 36, F117.	2.1	9
120	Plasmonic sensors based on nano-holes: technology and integration. Proceedings of SPIE, 2008, , .	0.8	8
121	Probing speciation inside a conducting polymer matrix by in situ spectroelectrochemistry. Electrochimica Acta, 2011, 56, 3101-3107.	5.2	8
122	Evaluation of Surface-Enhanced Raman Spectroscopy Substrates from Single-Molecule Statistics. Journal of Physical Chemistry C, 2017, 121, 25487-25493.	3.1	8
123	Nanostructuring Solar Cells Using Metallic Nanoparticles. , 2019, , 197-221.		8
124	Single-Molecule SERS Hotspot Dynamics in Both Dry and Aqueous Environments. Journal of Physical Chemistry C, 2022, 126, 7117-7126.	3.1	8
125	In situ micro Raman investigation of electrochemically formed halide and pseudohalide films on mercury electrodes. Journal of Raman Spectroscopy, 2002, 33, 136-141.	2.5	7
126	Raman maps reveal heterogeneous hydrogenation on carbon materials. Journal of Raman Spectroscopy, 2021, 52, 516-524.	2.5	7

#	Article	IF	CITATIONS
127	Protoporphyrin-modified gold surfaces for the selective monitoring of catecholamines. Electrochimica Acta, 2007, 52, 3863-3869.	5.2	6
128	Polarization-dependent extraordinary optical transmission from upconversion nanoparticles. Nanoscale, 2015, 7, 18250-18258.	5.6	6
129	From Dermal Patch to Implants—Applications of Biocomposites in Living Tissues. Molecules, 2020, 25, 507.	3.8	6
130	Nanotechnology Driven Cancer Chemoradiation: Exploiting the Full Potential of Radiotherapy with a Unique Combination of Gold Nanoparticles and Bleomycin. Pharmaceutics, 2022, 14, 233.	4.5	6
131	The adsorption and orientation of pyrazine on silver electrodes: a surface enhanced Raman scattering study. Journal of Electroanalytical Chemistry, 1996, 414, 183-196.	3.8	5
132	Development of plasmonic substrates for biosensing. Proceedings of SPIE, 2008, , .	0.8	5
133	Layer-by-Layer Characterization of a Model Biofuel Cell Anode by (in Situ) Vibrational Spectroscopy. Journal of Physical Chemistry C, 2011, 115, 310-316.	3.1	5
134	Template-Stripping Fabricated Plasmonic Nanogratings for Chemical Sensing. Plasmonics, 2018, 13, 231-237.	3.4	5
135	Plasmonic Light-Trapping Concept for Nanoabsorber Photovoltaics. ACS Applied Energy Materials, 2019, 2, 2255-2262.	5.1	5
136	Peering into the Formation of Template-Free Hierarchical Flowerlike Nanostructures of SrTiO <sub>3</sub> . ACS Omega, 2020, 5, 33007-33016.	3.5	5
137	Plasmonic linewidth narrowing by encapsulation in a dispersive absorbing material. Physical Review Research, 2021, 3, .	3.6	5
138	Quantification of a COVID-19 Antibody Assay Using a Lateral Flow Test and a Cell Phone. Chemosensors, 2022, 10, 234.	3.6	5
139	Microfluidic and nanofluidic integration of plasmonic substrates for biosensing. Proceedings of SPIE, 2009, , .	0.8	4
140	Sensing of antibodies secreted by microfluidically trapped cells via extraordinary optical transmission through nanohole arrays. , 2010, , .		4
141	Engineering of CdTe Multicore in ZnO Nanoshell as a New Charge-Transfer Material. Journal of Physical Chemistry C, 2014, 118, 18372-18376.	3.1	4
142	Large Area Plasmonic Gold Nanopillar 3-D Electrodes. Electrochimica Acta, 2016, 188, 91-97.	5.2	4
143	The development of surface-plasmon-based sensors using arrays of sub-wavelength holes. , 2005, 6002, 31.		3

Biaxial nanohole array sensing and optofluidic integration. , 2008, , .

#	Article	IF	CITATIONS
145	Controlling the Photoluminescence from a Laser Dye through the Oxidation Level of Polypyrrole. Macromolecular Rapid Communications, 2010, 31, 289-294.	3.9	3
146	Selective suppression of {112} anatase facets by fluorination for enhanced TiO <sub>2</sub> particle size and phase stability at elevated temperatures. Nanoscale Advances, 2021, 3, 6223-6230.	4.6	3
147	Dynamics of D2 released from the dissociation of D2O on a zirconium surface. Journal of Chemical Physics, 2006, 124, 124704.	3.0	2
148	Creating and fixing a metal nanoparticle layer on the holes of microstructured fibers for plasmonic applications. , 2008, , .		2
149	Electrokinetically-Induced Flow Over a Nano-Hole Array Sensor. , 2004, , 213.		1
150	Angle-dependent SHG enhancement from nanoscale doublehole arrays in a gold film. Journal of Physics: Conference Series, 2007, 61, 693-697.	0.4	1
151	Nanohole Arrays in Metal Films as Integrated Chemical Sensors and Biosensors. Springer Series on Chemical Sensors and Biosensors, 2010, , 155-179.	0.5	1
152	Analysis of SERS Reproducibility on Nanoparticle Microarrays. , 2010, , .		1
153	Double nanohole-enhanced Raman spectroscopy. , 2007, , .		Ο
154	Double nanohole-enhanced Raman spectroscopy. , 2007, , .		0
155	Nanohole Arrays as Optical and Fluidic Elements for Sensing. , 2008, , .		Ο
156	Real-time monitoring of self-assembled monolayer using biaxial nanohole arrays. , 2009, , .		0
157	Development of portable SPR sensor devices based on integrated periodic arrays of nanoholes. Proceedings of SPIE, 2009, , .	0.8	0
158	Handheld nanohole array surface plasmon resonance sensing platform. , 2010, , .		0
159	Multilayer Silver Nanoparticles Modified Optical Fiber Tip for High Performance SERS Remote Sensing. ECS Meeting Abstracts, 2010, , .	0.0	0
160	Nanofluidics Meets Plasmonics: Flow-Through Surface-Based Sensing. , 2010, , .		0
161	Nanoplasmonics as nanofluidics: transport and sensing in flowthrough nanohole arrays. , 2011, , .		0
162	Digital plasmonic holography with iterative phase retrieval for sensing. Optics Express, 2021, 29, 3026.	3.4	0

0

#	Article	IF	CITATIONS
163	Integration and Application of a Surface Plasmon Sensor Array On-Chip. , 2006, , .		0

164 Flow-Through Nanohole Array Based Sensing. , 2009, , .